

Infrared and EPR studies of the red potassium molybdenum bronze $K_{0.33}MoO_3$

RUI XIONG, JING SHI*, QINGMING XIAO, WUFENG TANG, HAILING LIU, DECHENG TIAN

Department of Physics, Wuhan University, Wuhan, 430072, People's Republic of China
E-mail: labcdw@whu.edu.cn

Infrared reflectance and electron-paramagnetic-resonance (EPR) of the red bronze $K_{0.33}MoO_3$ are presented. The infrared measurements at 300 K indicated that red bronze $K_{0.33}MoO_3$ is a semiconductor with very strong anisotropy in the range. The presence of three sharp lines at about 900 cm^{-1} for $P \perp b$ is in fact due to the intramolecular oscillations of oxygen inside one octahedron. The phonon oscillators near 500 cm^{-1} for $P \perp b$ and $P \parallel b$ associate with the modification of the effective charge. The EPR signals can be attributed to electrons localized in the isolated Mo^{5+} paramagnetic center. The difference of relative intensities of the EPR lines in 300 K and 100 K is due to the electronic excitation. The inhomogeneous broadening of the resonance lines is due to a g -factor distribution arising from crystalline field and spin-orbit coupling. © 2001 Kluwer Academic Publishers

1. Introduction

Among the series of potassium molybdenum bronzes of general formula $K_xMo_yO_z$, two compounds, the blue bronze $K_{0.3}MoO_3$ and the purple bronze KMo_6O_{17} , have been extensively studied due to the extremely rich variety of properties [1–3]. The blue bronze $K_{0.3}MoO_3$ exhibits a metal to semiconductor (CDW) transition at 180 K with the formation of the charge density wave (CDW). The crystal structure of blue bronze $K_{0.3}MoO_3$ is monoclinic with 20 formula per unit cell (space group $c2/m$) and is built of infinite sheets of distorted MoO_6 octahedra held together with the K cations. The MoO_6 layers consist of clusters of ten edge-sharing octahedra linked by corners in the [010] and [102] directions [4, 5]. The purple bronze KMo_6O_{17} is a quasi-two-dimensional conductor which undergoes a CDW transition at about 120 K due to the nesting of hidden Fermi surfaces. The crystal structure of purple bronze KMo_6O_{17} is trigonal with space group $P3$. The ideal structure of KMo_6O_{17} can be described in terms of slabs of Mo–O corner-sharing polyhedra. Each slab of Mo–O polyhedra consists of four layers MoO_6 octahedra sharing corners, which are terminated on either side by a layer of MoO_4 tetrahedra sharing corners with adjacent MoO_6 octahedra in the same layer. These slabs are perpendicular to the c -direction and are separated from each other by a layer of monovalent metallic ions in a KO_{12} icosahedral environment of oxygen [6–8]. A third compound, the red bronze $K_{0.33}MoO_3$, has been shown to be at all temperature a semiconductor [9]. The monoclinic structure (space group $c2/m$) of red bronze, determined by Stephenson and Wadsley [10], is built of infinite sheets of corners/edge-sharing distorted MoO_6

octahedra joined together by the K^+ ions which are in an irregular eightfold coordination. The structure of the red bronze is very similar to that of the blue bronze except that in the red bronze the unit of structure is six edge-shared octahedra, which then corner share along b and the [102] direction to form the infinite layers.

Although CDW transition doesn't exist in red bronze $K_{0.33}MoO_3$, the studies of the red bronze can help us clarify some of the ambiguities in the study of the series of molybdenum bronzes due to the electronic structural similarity of these series. On the other hand, the interpretations of experimental situation remained controversial. For this reason, we discuss the infrared reflectivity and EPR measurement from single crystal of $K_{0.33}MoO_3$.

2. Experimental procedure

Single crystals of potassium red molybdenum oxide bronze were grown by the electrolytic reduction of a melt of K_2CO_3 - MoO_3 with molar ratio of $K_2CO_3:MoO_3 = 1:3.3$. Temperature, melt composition and current density control the product phase [11]. The resulting crystals are red platelets of typical size $6 \times 5 \times 0.5\text{ mm}^3$. The temperature dependence of the resistivity from 300 K to 150 K established the semiconductor behavior of this compound. The structure and the composition were identified by single-crystal X-ray diffraction technique and analysis of X-ray photoelectron spectra, respectively. The results will be described in detail elsewhere.

The optical reflectivity of single crystals of $K_{0.33}MoO_3$ in infrared scale was measured by comparing

*Author to whom all correspondence should be addressed.

the intensity of reflecting light and the incident light with the incident light being polarized parallel or perpendicular to b direction in the a - b plane. The crystallographic b axis was found by turning the polarization of incident light until the reflectivity reached a maximum for a given wavelength. The EPR spectra in 300 K and 100 K have been carried out on samples of typical size $6 \times 5 \times 0.5 \text{ mm}^3$ using an x band Bruker ER-200 D-SRC spectrometer operating with a 100 kHz field modulation. The magnetic field kept perpendicular to a - b plane, and ranged from 0 Gs and 8000 Gs.

3. Results

3.1. Infrared polarized reflectivity spectra

The polarized reflectivity spectra in the infrared range with the polarization parallel to b ($P \parallel b$) and perpendicular to b ($P \perp b$) at 300 K are shown in Figs 1 and 2.

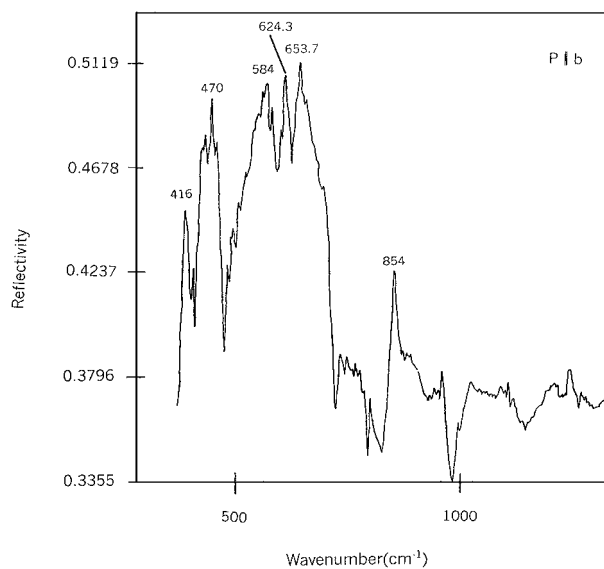


Figure 1 The polarized reflectivity spectra in the infrared range of red bronze $\text{K}_{0.33}\text{MoO}_3$ with the polarization parallel to b -axis ($P \parallel b$) at 300 K.

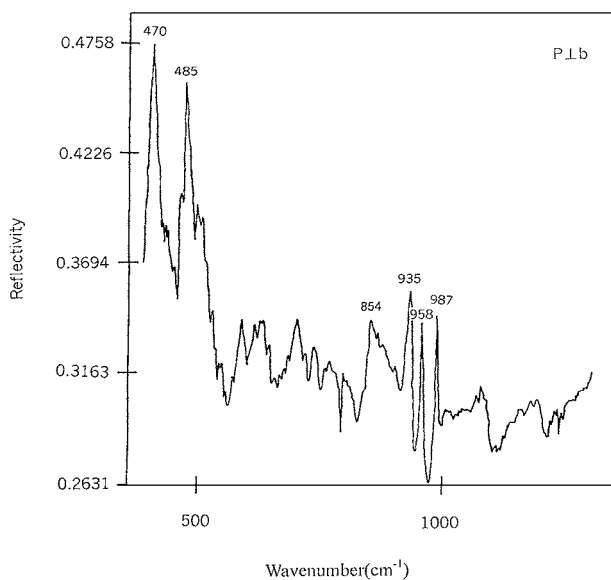


Figure 2 The polarized reflectivity spectra in the infrared range of red bronze $\text{K}_{0.33}\text{MoO}_3$ with the polarization perpendicular to b ($P \perp b$) at 300 K.

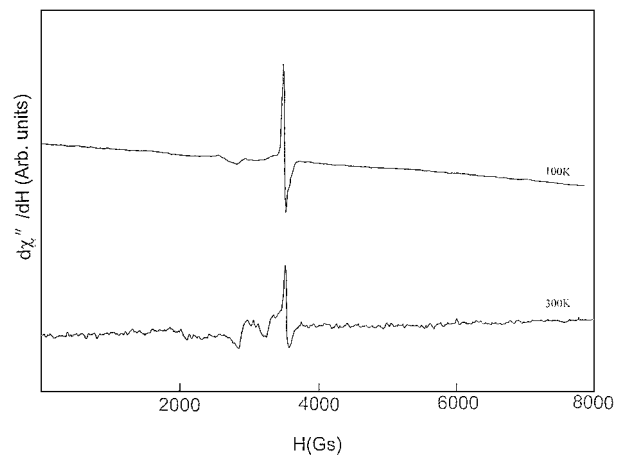


Figure 3 The EPR spectra of red bronze $\text{K}_{0.33}\text{MoO}_3$ at 300 K and 100 K, $d\chi''/dH$ values are corresponding to the relative energy absorption from the microwave magnetic field due to the electron transition from Mo^{5+} donor levels.

It is obvious that both polarized reflectivity spectra are semiconductor-like but with different intensities and resonance. Many sharp lines due to phonon absorption are observed for photo energies in the infrared range. A realistic phonon analysis for this material is very difficult because of the large number of atoms in the primitive unit cell ($4_{\text{K}} + 12_{\text{Mo}} + 36_{\text{O}} = 52$ atoms). One expects approximately 60 infrared as well as Raman active modes belong to the representation A_u , B_u , A_g and B_g for the space group $c2/m$, respectively.

3.2. Electron-paramagnetic-resonance spectra

The EPR spectra of red bronze $\text{K}_{0.33}\text{MoO}_3$ at 300 K and 100 K are shown in Fig. 3. Both spectra have a paramagnetic resonance peak; but the relative intensities and Lande factor g of lines varied with the temperature. The Lande factor g is 1.971 at 300 K and 1.957 at 100 K, and the resolution of line width of the two peaks is 55 Gs at 300 K and 35 Gs at 100 K. A similar signal has also been observed for red bronze $\text{K}_{0.33}\text{MoO}_3$ with g value 1.96 and line width of 40 Gs in the measurement of the electron-spin-resonance (ESR) by Dichen *et al.* [12]. It seems reasonable to associate the signals with the presence of Mo^{5+} active sites.

4. Discussion

The electronic structures of molybdenum bronzes can be interpreted as follows: $5p$, $5s$ and $4d$ (e_g) cationic orbitals combine with the $2s$ and $2p_\sigma$ anionic orbitals to form an occupied bonding σ valence band and an empty anti-bonding σ^* band, with significant $d(e_g)$ character. The $4d$ (t_{2g}) cationic orbitals combine with the $2p_\pi$ anionic orbitals to give a bonding π valence band and an anti-bonding π^* conduction band [13]; the $(\pi^* - \sigma^*)$ conduction—and the $(\pi - \sigma)$ valence bands are separated by the energy gap. Because of the octahedral crystal-field and the strong d -character the π^* and σ^* conduction bands are separate. The Mo atoms are incorporated as Mo^{5+} ions giving rise to a corresponding number of

n electrons pro formula unit in the lower lying and otherwise empty π^* -levels having strong d-character. The extent of delocalization of the d-electrons characterize the transport- and optical properties of molybdenum bronzes. Mo^{5+} orbitals do not contribute to the formation of these levels as confirmed by several experiments [14, 15], but to the formation of the donor levels located between the valence and conduction bands of the MoO_3 matrix. It is suggested that electrons originating from the alkali metals are trapped at these donor levels.

The strong anisotropy of the signal in the infrared range is due to two different characters A_u and B_u of the phonons and since the clusters are constructed by six MoO_6 distorted octahedra, both kind of phonons can be present in every of the two polarized spectra. Strong phonons are present in triplets around 900 cm^{-1} for $P \perp b$ while they are not detected for $P \parallel b$. These strong triplets are also observed in the blue bronze $\text{K}_{0.3}\text{MoO}_3$ [16, 17], purple bronze $\text{KMo}_6\text{O}_{17}$ [18] and in the oxide MoO_3 [19], and have been wrongly interpreted as transitions between different Mo sites in blue bronzes and purple bronzes due to the three nonequivalent positions of molybdenum atoms in the structure [16]. Because only the blue bronzes and purple bronzes has three 3 Mo sites, the red bronze has 2 sites and MoO_3 1 site. Considering the octahedron distortion, it turns out that a tetragonal distortion with a lower symmetry (point group C_4) could explain this absorption triplet. Since all these compounds have octahedra as building units, it is in fact the intramolecular oscillations of oxygen inside one octahedra give rise to these three sharp lines. The octahedron point group O_h contains a triple degenerate T_{1u} mode and since the octahedra in these materials are distorted, this mode splits in three lines of the kind T_{1u} .

It is noticeable that three strong phonon peaks are presented near 584 , 624 and 654 cm^{-1} for $P \parallel b$, while they are presented lower for $P \perp b$. These phonons have not been reported in document [20]. The origins of these phonons remain not clear, however it must relate to the anisotropic structure of the red bronze.

In the vicinity of 500 cm^{-1} for $P \perp b$ (485 cm^{-1}) and $P \parallel b$ (470 cm^{-1}), strong phonon oscillator was observed. The oscillator has been reported in blue bronze $\text{K}_{0.3}\text{MoO}_3$ and has been attributed to mid-Peierls-gap states in a direction where a normal semiconducting gap exists with no Peierls gap [16]. However, such an oscillator is observed in red bronze $\text{K}_{0.33}\text{MoO}_3$ for both $P \perp b$ and $P \parallel b$ where Peierls transition can not occur. Comparison of phonon parameters at 300 K with those at 9 K reported in blue bronzes $\text{K}_{0.3}\text{MoO}_3$ [17] does not indicate a noticeable effect of the CDW on the phonon frequencies. Nevertheless, the oscillator strength of phonons with frequency is affected and markedly modified at low temperature, indicating a modification of the effective charge associated with these vibrations.

In the EPR spectra, the observation of signals at room temperature is again consistent with the proposal that the Mo^{5+} donor levels for the red potassium bronze lies extremely lower than the blue potassium bronze between the valence and conduction bands. An important observation is that, at low temperature the reso-

nance line is sharp and well resolved, while at elevated temperature the spectrum is complicated and poor of resolution. The temperature dependence of resonance spectra has also been reported in blue bronze $\text{A}_{0.3}\text{MoO}_3$ ($A = \text{K}, \text{Rb}, \text{Tl}$) [21, 22]. It has been proposed that this phenomenon be related to the thermal history and the relaxation properties of metastable behavior. We suggest that the basic origin be due to the electrons exciting into the delocalized band from Mo^{5+} sites at elevated temperature. Only at low temperature where electrons are localized in isolated Mo^{5+} donor levels does a well-resolved EPR signal appear. The increasing loss of resolution of signal with increasing temperature for the blue potassium bronze below 180 K has the same origin.

The inhomogeneous broadening is due to a g -factor distribution. The Mo^{5+} ion may be described as a single d electron in a distorted octahedral environment [23]. The relative difference of the g factor from the free-electron value of about $\Delta g/g \sim 5 \times 10^{-2}$ arises from the crystalline field and spin-orbit coupling. Thus a g -factor distribution can be observed by EPR measurement. This is also valid for the observed inhomogeneous broadening of g -factor in blue bronze $\text{A}_{0.3}\text{MoO}_3$ ($A = \text{K}, \text{Rb}, \text{Tl}$).

5. Conclusion

In conclusion, we find that the infrared reflectance and EPR studies of $\text{K}_{0.33}\text{MoO}_3$ can allow us to clarify some of the ambiguities in the study of the series of molybdenum bronzes. The anisotropic and semiconducting character of the red bronze $\text{K}_{0.3}\text{MoO}_3$ can also be demonstrated in our infrared and EPR studies.

The observation of phonon lines at about 900 cm^{-1} and 500 cm^{-1} in our experiment demonstrates that these phonon lines have nothing to do with the CDW state. The EPR signals can be attributed to electrons that are localized in the isolated Mo^{5+} paramagnetic center. The difference of relative intensities of the EPR lines in 300 K and 100 K is due to the electronic excitation, and the inhomogeneous broadening of the resonance line is due to a g -factor distribution arises from the crystalline field and spin-orbit coupling.

Acknowledgement

The authors thank the Chinese Foundation of Natural Science for financial support (No. 59872023).

References

1. G. GRUNER, *Rev. Mod. Phys.* **32** (1998) 1129.
2. J. DUMAS and C. SCHLENKER, *Int. J. Mod. Phys.* **B7** (1993) 4045.
3. M. GREENBLATT, *Chem. Rev.* **88** (1988) 31.
4. W. FOGLE and J. H. PERLSTEIN, *Phys. Rev. B* **6** (1972) 1402.
5. J. DUMAS, C. SCHLENKER, J. MARCUS and R. BUDER, *Phys. Rev. Lett.* **50** (1983) 7547.
6. H. VINCENT, M. CHEDIRA, J. MARCUS, J. MERCIER and C. SCHLENKER, *J. Solid State Chem.* **47** (1983) 113.
7. M. ONADA, Y. MATSUDA and M. SATO, *ibid.* **69** (1987) 67.
8. M. GANNE, M. DION, A. BOUMAZA and M. TOURNOUX, *Solid State Commun.* **59** (1986) 137.
9. G. H. BOUCHARD, J. H. PERLSTEIN and M. J. SIENKO, *Inorg. Chem.* **6** (1967) 1682.

10. N. G. STEPHENSON and A. D. WADSLEY, *Acta Cryst.* **18** (1965) 241.
11. Z. HUANG, M. L. TIAN and D. C. TIAN, *J. Low. Temp. Phys.* **12** (1990) 78.
12. P. G. D. CKENS and D. J. NEILD, *Trans. Faraday Soc.* **64** (1968) 13.
13. G. TRAVAGLINI, P. WACHTER, J. MARCUS and C. SCHLENKER, *Solid State Commun.* **37** (1981) 599.
14. G. SPERLISH, *Z. Physik* **250** (1972) 335.
15. V. A. JOFFE and I. V. PATRINA, *Sov. Phys. Sol. State* **10** (1968) 639.
16. N. E. MASSA, *Phys. Rev. B* **34**(8) (1986) 5943.
17. S. JANDL, M. BANVILLE, C. PEPIN, J. MARCUS and C. SCHLENKER, *ibid.* **40**(18) (1988) 12487.
18. L. DEGIORGI, P. WACHTER, M. GREENBLATT, W. H. MCCARROLL, K. V. RAMANUJACHARY, J. MARCUS and C. SCHLENKER, *ibid.* **38** (1988) 5821.
19. M. A. PY and K. MASCHKE, *Physica B + C* **105B** (1981) 370.
20. G. TRAVAGLINI, P. WACHTER, J. MARCUS and C. SCHLENKER, *Solid State Commun.* **42**(6) (1982) 407.
21. J. DUMAS, B. LAAYADI and R. BUDER, *ibid.* **72**(5) (1989) 429.
22. J. DUMAS, R. BUDER, J. MARCUS, C. SCHIENKER and A. JANOSSY, *Physica* **143B** (1986) 183.
23. G. BANG and G. SPERLICH, *Z. Physik B* **22** (1975) 1.

*Received 21 April 2000
and accepted 3 August 2001*